Egypt. J. Chem. **Vol. 65,** No. SI:13, pp. 791 - 805 (2022)

Egyptian Journal of Chemistry

http://ejchem.journals.ekb.eg/

Desulfurization of Initial Sulfur Compounds in Diesel Fuel by Oxidation-Emulsification Processes

Ahmed A. Hantosh, Adnan A. AbdulRazak* and Adel Sharif Hamadi

Chemical Engineering Department, University of Technology, Baghdad, Iraq.

Abstract

In the present study, the combined oxidation–emulsification was used to desulfurize diesel fuel with a hydrogen peroxide–acetic acid oxidation system. A full 20 central composite design response surface method was employed to study the effect of 5-20% oxidant range, 40-100°C temperature range and 20-90 min time. A 0.781% sulfur content was obtained at 12.5 wt% oxidant ratio, 65°C temperature 60 min via the oxidation process. The effect of emulsification desulfurization on oxidized diesel fuel was investigated using five surfactants: cetyltrimethylammonium chloride (cationic), nonylphenol ethoxylates (nonionic), alkylbenzene sulfonate (anionic), tween 80 (nonionic), and 1-hyroxy-2-(trimethylammonio) ethane-1-sulfonate (Amphoteric). A 0.598% sulfur content was obtained using alkylbenzene sulfonate. The desulfurize diesel fuel was charactizied using GC-MASS, IREX, and FTIR. The results indicated that the combined oxidation–emulsification process may be used to desulfurize diesel.

Keywords: Oxidation; emulsification; desulfurization; diesel fuel; response surface; surfactant.

1. Introduction

Energy is a major driving force for progress, and diesel is widely used as a primary fuel source worldwide. However, the high sulfur concentration in this fuel produces a significant amount of hazardous emissions into the environment[1]. Controlling sulfur content in fuels is a major priority for governments in this regard, with numerous technologists and tight legislation helping to lower it to safe levels[2]. High concentrations of sulfur compounds cause significant health concerns in humans. For example, a human was carcinogenic after being exposed to a specified quantity of heavier thiophene[3]. Thiols with a foul odor induce respiratory issues such as breathing difficulties, throat and lung irritation, aggravation of the eyes, muscular spasms, and unconsciousness. Increases in the quantity of sulfur compounds in the environment contribute to atmospheric contamination and lower air quality[3]. Sulfur dioxide is a significant pollutant created when sulfur atoms combine with oxygen during burning, posing the organisms through acid rain and photochemical fog[4]. Authorities in developed nations use regulations to control the sulfur concentration in fossil fuels due to pollution and human health concerns during combustion. These rules become much tougher with time, particularly in the United States and the European Union[3]. This is a direct outcome of the stringent environmental regulations. It limits the sulfur amount in fuel to less than 15 µg/g since 2006 in the US, under 10 µg/g since 2005 in Europe, and under 50 µg/g since 2008 in Beijing and Shanghai in China[5-7].

The most widely used method for sulfur removal is hydrogenation, which requires severe working conditions and an expensive catalyst[8]. Hydrodesulfurization (HDS) has been used in industry for a long time because it is extremely effective in removing thiols, sulfides, and disulfides from fuels[9]. However, due to refractory sulfur in diesel fuel, the hydrodesulfurization method is not very successful in removing 4,6-dimethyl dibenzothiophene (4,6-DMDBT) and its derivatives[10, 11]. The primary disadvantages of the HDS process are the high pressure (20-60 bars) and temperature (593-673 K)

*Corresponding author e-mail: adnan.a.alsalim@grad.uotechnology.edu.iq.; (Adnan A. AbdulRazak).
Receive Date: 15 February 2022, **Revise Date:** 12 March 2022, **Accept Date:** 26 March 2022,
First Publish Date: 14 November 2022
DOI: 10.21608/EJCHEM.2022.121709.5466

requirements, the considerable amount of H_2 gas required, and the method's inefficiency with refractory sulfur compounds[12].

Desulfurizations that have been explored recently include oxidation, extraction, biological techniques, and adsorption[13]. The literature on desulfurization processes shows that the nontraditional method of removing sulfur from oil fractions is oxidative desulfurization[14-21].

The oxidation of divalent sulfur to hexavalent sulfur in sulfones is much different than that of hydrocarbon molecules, resulting in molecules with radically distinct physical and chemical properties[11]. Hydrogen peroxide (H_2O_2) was an excellent option for oxidation due to its large mass unit (47 percent) of active oxygen. A catalyst is required to oxidize the sulfur compounds successfully. This commercial component produces water, widely utilized in the industry[22]. Recent investigations on desulfurization have identified numerous oxidation systems, including acetic acid/H_2O_2[23, 24], formic acid/H_2O_2[24, 25], heteropoly acid/H_2O_2 [26, 27], polyoxometalates/OO_2 [28, 29], aldehyde/O_2 [30, 31], and TS-1/H_2O_2[32, 33]. The oxidation of sulfur dioxide with H_2O_2 is a promising desulfurization process because it produces just water as a by-product and does not pollute the environment. Catalysts, such as organic solvents, and surfactants, are used in oxidation with H_2O_2 to boost the reactivity of desulfurization and prevent ODS processes from being inhibited, as they are always two- or three-phase processes[34, 35]. Some researchers are studying the phase transfer catalysts in ODS due to the immiscibility of the two reaction phases: the polar phase containing H_2O_2 and the nonpolar oil phase containing sulfur compound[36, 37].

Microemulsions are optically clear, thermodynamically stable, low interfacial tension, low viscosity, homogeneous, and high capacity for pollutant solubilization[38]. This system results from the dispersion of two immiscible liquid phases using a high or low energy method, with or without the presence of a co-surfactant[39, 40]. The surfactants reduce the interfacial tension of these liquids. Surfactants are amphiphilic molecules formed of two parts: polar hydrophilic (head group) and nonpolar hydrophobic (tail group) groups[41]. Due to the dispersed droplet size, the emulsified fuel increases mass transfer between the two phases, resulting in a large interfacial area and a shorter equilibrium time. Emulsification is often accomplished using high-speed mechanical energy or through surfactants to reduce interfacial and surface tension[39, 42].

This research presents a study of the desulfurization of diesel fuel by the combined oxidation–emulsification technique.

2. Experimental

2.1. Materials

Desulfurization was carried out using non-hydrotreated diesel feedstock supplied by the Basra refinery with a total sulfur level of 0.945 wt%. The diesel fuel proprieties are listed in Table 1. Acetic acid 95% and Hydrogen peroxide 37% are obtained from the South Refineries Company lab. Table 2 lists the surfactants employed in the creation of emulsions, all the surfactants supplied from vegetable oils company-Iraq.

Table 1. Specifications of diesel oil.

Propriety	ASTM Method	Result
Aspect (visual)	D4176	Clear and free of impurities
Colour	D1500-64	Zero
Total Sulfur (wt%)	D4294	0.945
Cetane number	D4737	34.7
Specific gravity at 20ºC (g/cm^3)	D4052	0.8214
Ash (wt.%)	D482	<0.0011
Viscosity at 40°C (mm^2.s^{-1})	D445	1.8678
Sediment and water (% volume)	D2709	0.0096
Flash point (ºC)	D93	72

Table 2. Used surfactants for the emulsification process.

Surfactant	Type	Source
Cetyltrimethylammonium Chloride (CAC)	Cationic	Vegetable oils company-Iraq
Nonylphenol ethoxylates (NPE)	Nonionic	Vegetable oils company-Iraq
Alkyl benzene sulfonate (ABS)	Anionic	Vegetable oils company-Iraq
Tween 80 (T80)	Nonionic	CDH company
1-hyroxy-2-(trimethylammonio) ethane-1-sulfonate (HES)	Amphoteric	Vegetable oils company-Iraq

2.2. Oxidation and emulsification of diesel fuel

The oxidation of Basra diesel fuel was done in a 500 ml conical flask with an electric stirrer. Hydrogen peroxide and acetic acid were mixed at a 2:1 ratio to prepare peracetic acid, added to diesel fuel. Eventually, the mixture was stirred at the desired conditions. Three factors of time, temperature, and %oxidant were optimized by the Design software process for discovering the optimum process conditions.

A high-speed homogenizer conducted the emulsification of oxidized diesel at the optimum conditions in a test tube. The first addition of 10 wt% water, 2 wt% surfactants, and 18 wt% of 2-propanol on diesel fuel, then homogenizing the mixture at 15000 rpm for 10 minutes. The water droplets in emulsified fuel were depicted by the NOVEL microscopy model (XSZ-N107), as shown in Figure 1.

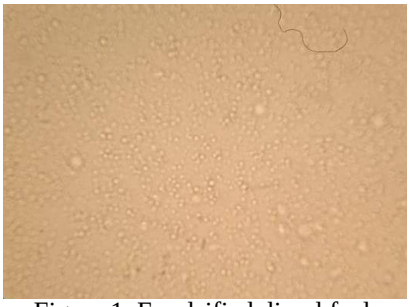

Figure 1. Emulsified diesel fuel.

After centrifuging the mixture, it was allowed to cool to ambient temperature. Figure 2 illustrates the centrifuge separation of emulsified fuel. A sample of 50 mL treated diesel fuel was taken to determine the total sulfur concentration. The desulfurization rate was determined using Eq. 1 using the initial and final sulfur concentration before and after treatment.

$$Rate\ of\ desulfurization = \frac{S_{initial} - S_{final}}{S_{initial}}(100) \quad (1)$$

Where: $S_{initial}$ and S_{final} are the sulfur content in net diesel fuel and after the treatment.

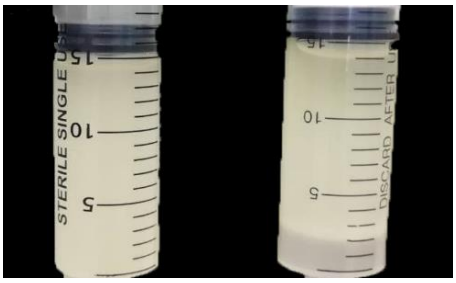

(a) Before centrifuge (b) After cetrifuge

Figure 2. Emulsified diesel fuel Separation before and after centrifuge.

2.3. Method of analysis

Sulfur content

The total sulfur concentration of the feedstock and treated samples was determined using the HORIBA sulfur analyzer "SLFA-2100, Japan," which used the energy dispersive X-ray fluorescence technology to follow the "ASTM D-4294" standard.

Gas Chromatography

Sulfur compounds were detected by using Trace sulfur analyzer (Sulfur Gas Analyzer – Model 4629, USA) by sulfur chemiluminescence detector (SCD) according to the "ASTM D-5504 and ASTM D-5623" method.

IREX analysis

Concentrations of all relevant fuel components in diesel fuel before/after desulfurization were accomplished using a spectral fuel analyzer (eraspec, Austria) based on the ASTM D-5845, D-6277, D-7777, D-7806, EN-238, EN-14078, ISO-15212, and IP559 standards.

FTIR Test

Chemical bonds within a molecule are identified by producing an infrared absorption spectrum for fuels prior to desulfurization using PerkinElmer Frontier IR/NIR systems, USA, based on Fourier Transform Infrared Spectroscopy (FTIR).

2.4. Design of Experiments

An experimental design can determine and assess the interaction and contribution of parameters to the attained goals. Models may also provide optimization of interacting parameters based on the desired results. The "Response Surface Methodology (RSM)" was used to evaluate the influences of chosen oxidation variables utilizing the Central Composite Design (CCD) approach. Experiments in this study are designed using the CCD approach on three levels (-1, 0, and +1). The experimental limits and factor levels are summarized in Table 3. The oxidation process is optimized and modelled using Design-Expert software version 10.0.7 to get the desired output values. This procedure oxidizes sulfur compounds to sulfones in order to lower the sulfur content of diesel fuel.

Table 3. Parameters levels used in this work.

Symbol	Parameters	Unit	-1	0	+1
A	Time	Minutes	20	55	90
B	Temperature	Centigrade	40	70	100
C	Oxidant%	wt%	5	12.5	20

3. Results and discussion

3.1. RSM statistical and analytical analysis

Experiments and responses of three parameters (Temperature, time, and %oxidant) are tabulated in Table 1. All of the experiments were conducted on the same basis of weight equal to 100 gm.

Table 4. CCD experiments and the response values.

Run	Time (min)	Temperature(ºC)	Oxidant%(wt%)	Sulfur Content(wt%)
1	55	25	12.5	0.941
2	55	70	12.5	0.895
3	20	100	5	0.987
4	55	70	12.5	0.91
5	55	70	12.5	0.876
6	20	100	20	0.941
7	20	40	20	0.862
8	55	70	12.5	0.905
9	110	70	12.5	0.861
10	55	70	12.5	0.914
11	2.5	70	12.5	0.921
12	55	70	12.5	0.898
13	20	40	5	0.939
14	55	70	1.25	0.901
15	90	40	5	0.870
16	55	70	25	0.781
17	55	115	12.5	1.076
18	90	100	20	0.925
19	90	100	5	0.965
20	90	40	20	0.796

Based on the responses in Table 4, the minimum sulfur content (wt%) is obtained in run 16, equal to 0.781. Analysis of variance (ANOVA) is illusstrated in Table 5. A quadratic model is adopted to evaluate the significance of the parameters and determine the model competency by polynomial analysis. A empirical relation between output (Responses) and input variables in terms (temperature(A), time(B) and oxidant %(C) is approved by polynomial second order-quadratic for oxidization sulfur compound in equation 2:

$$\text{sulfur content (wt\%)} = +0.90-0.021*A+0.044*B -0.031*C+0.012*AB+0.001125*AC +0.008125*BC-0.00647*A^2 +0.045*B^2-0.025*C^2 \quad (2)$$

According to equation 2, the coefficient for time (A) registered (-0.021). The negativity of the parameter refers to attribution towards reducing the response wt% sulfur content. The positive coefficient of temperature (B) recorded (+0.044) shows that the temperature had a positive effect on wt% sulfur content. The coefficient recorded by % oxidant (C) is (-0.031) shows that the % oxidant had a negative effect on wt% sulfur content.

Table 5. ANOVA outcomes of the response surface quadratic model.

Source	Sum of Squares	Df	Mean square	F value	p-value Prob>F	
Model	0.076	9	0.0084	62.77	<0.0001	significant
A-Time	0.0054	1	0.0054	40.34	<0.0001	
B-Temperature	0.025	1	0.025	182.67	<0.0001	
C-oxidant %	0.013	1	0.013	93.18	<0.0001	
AB	0.00117	1	0.00117	8.77	0.0143	
AC	0.00001	1	0.00001	0.075	0.7891	
BC	0.00053	1	0.00053	3.94	0.0754	
A2	0.00046	1	0.00046	3.45	0.0930	
B2	0.021	1	0.021	155.10	<0.0001	
C2	0.0078	1	0.0078	58.08	<0.0001	
Residual	0.0013	10	0.00013			
Lack of Fit	0.000416	5	0.000083	0.45	0.7993	not significant
Pure Error	0.00092	5	0.00018			
Cor Total	0.077	19				

The model had an F-value of 62.77, showing appropriately selected and significance in this procedure. The F-statistic is essentially a ratio of two variances, derived by dividing the “regression mean square” by the “error term mean square”. Variances measure dispersion or the degree to which data deviate from the mean. Higher values indicate greater dispersion, with F equal to (difference between sample means/difference within samples).

The P-value indicates the likelihood that experiments may produce results as extreme as those seen by a statistical hypothesis test, given that the null hypothesis is accepted. When the P-value is less than 0.05, it indicates that the factor significantly affected the process. This investigation approved the model since the P-value is less than 0.05, indicating a substantial effect on response.

This model can use for optimization and prediction purposes because of lack of fit recorded 0.45 and obtained P-value 0.7933, which is not significant[43, 44].

The statistical parameters est
proposed model are shown in Table
of variation (C.V.) is 1.28%, indica
is reliable and the data is repeatable

Table 6. ANOVA statistical parame

Parameter	Value	Para
Std.Dev.	0.012	R-Sq
Mean	0.91	Adj R-S
C.V.%	1.28	Pred R-
PRESS	0.0042	Adeq P
-2Log Likelihood	-135.43	B
		AICc

The coefficient of determination R2 is 98.26%, which is consistent with the adjusted coefficient of determination adj- R2 of 96.7%; bo
to 1.0. These high values provide ev
between expected and determined v
of the variance in the depend
response) to the variance in the ind
(the predictors). It can be used t
performance, where adj- R2 reflec
fit a curve or line but accounts for th
in a model. We achieve a high valu
and adj- R2 (0. 9670) reasonably co

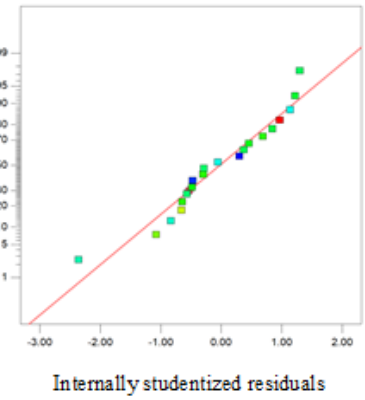

(a)

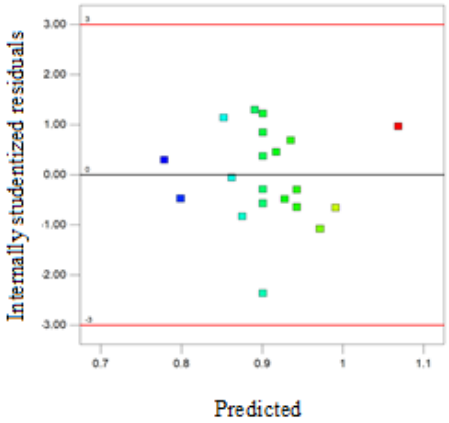

(c)

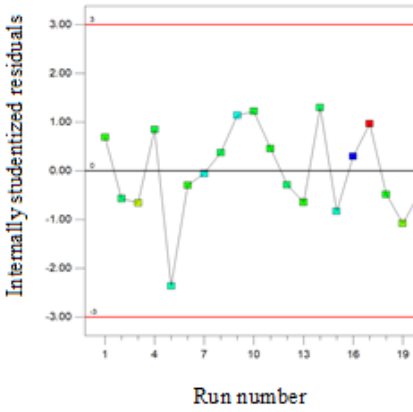

(d)

Figure 3 depicts the diagnostic plots for the data. These graphs could be used to examine the errors and residuals.

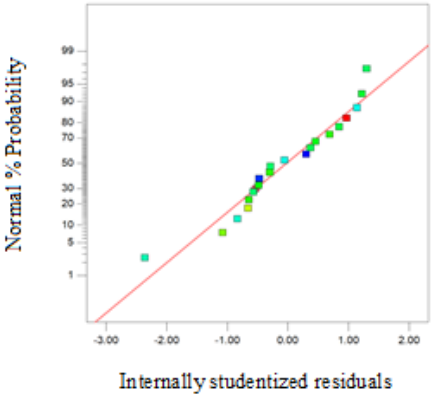

(a)

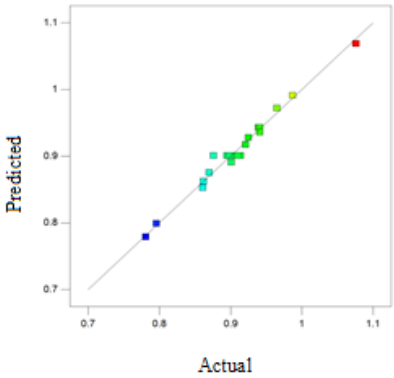

(b)

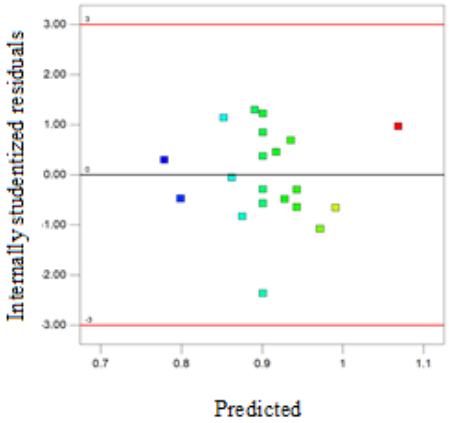

(c)

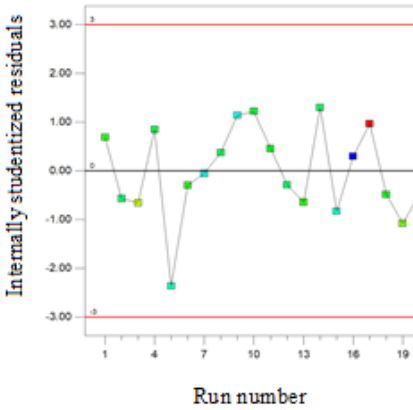

(d)

Figure 3a illustrates the normal plot of residuals. Although some data is dispersed, a straight line showing the normal residual distribution is followed. A graph depicting the quantities of actual and predicted response values is shown in

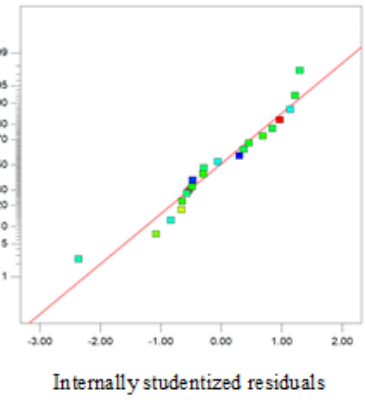

(a)

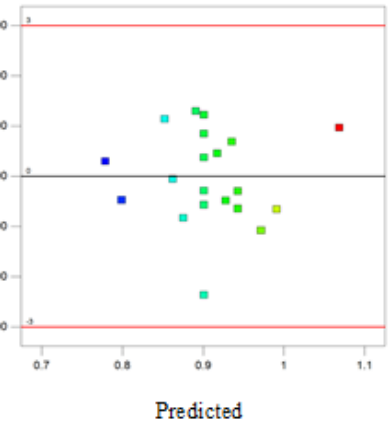

(c)

Figure 3b. It checks the
assumption and may be used to fi
prediction model predicts erroneously. The residual vs
the ascending anticipated response

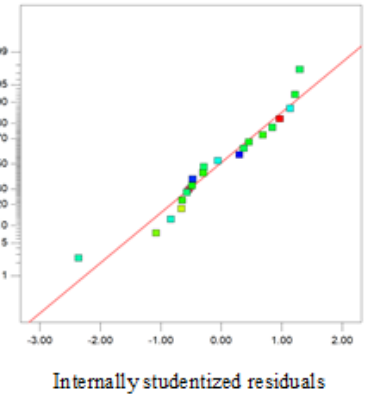

(a)

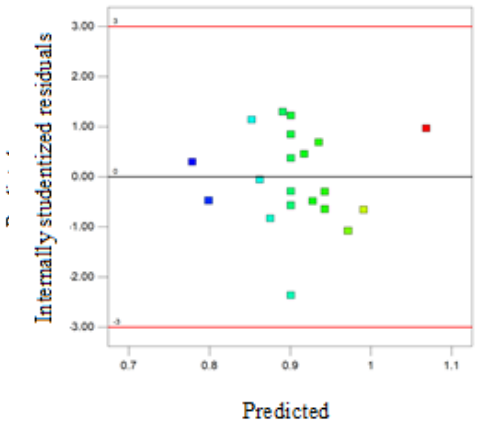

(c)

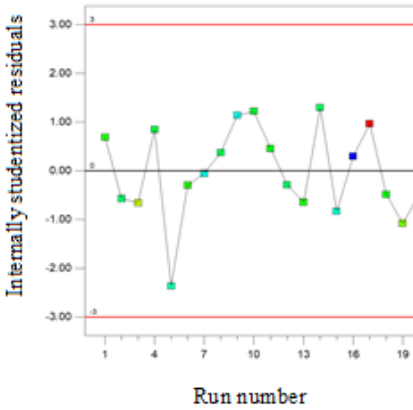

(d)

Figure 3c validates the constant variance assumption. The points are distributed randomly between a range of + 1 to -2.

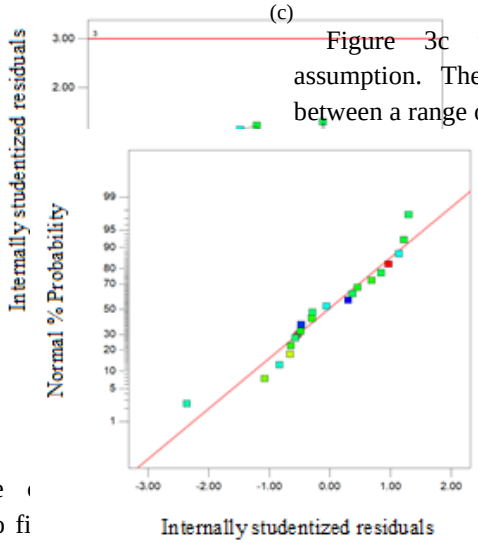

(a)

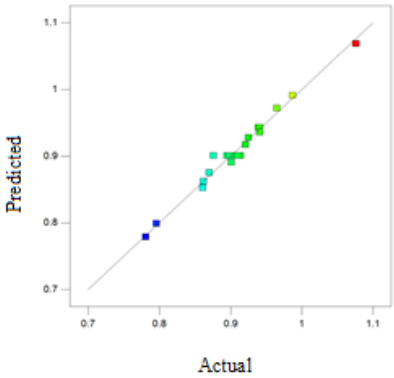

(b)

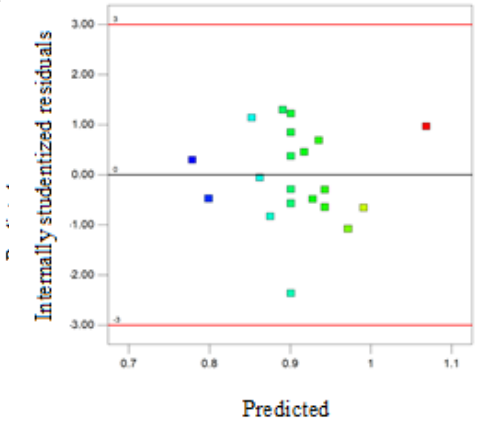

(b) (c)

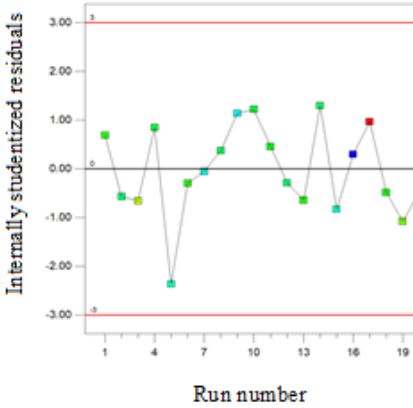

(d)

Figure 3d illustrates the run number versus residuals findings, which wiggle randomly around the zero line. The residue appears to be distributed randomly around the zero line. This shows that there is no evidence that the mistake phrases are connected.

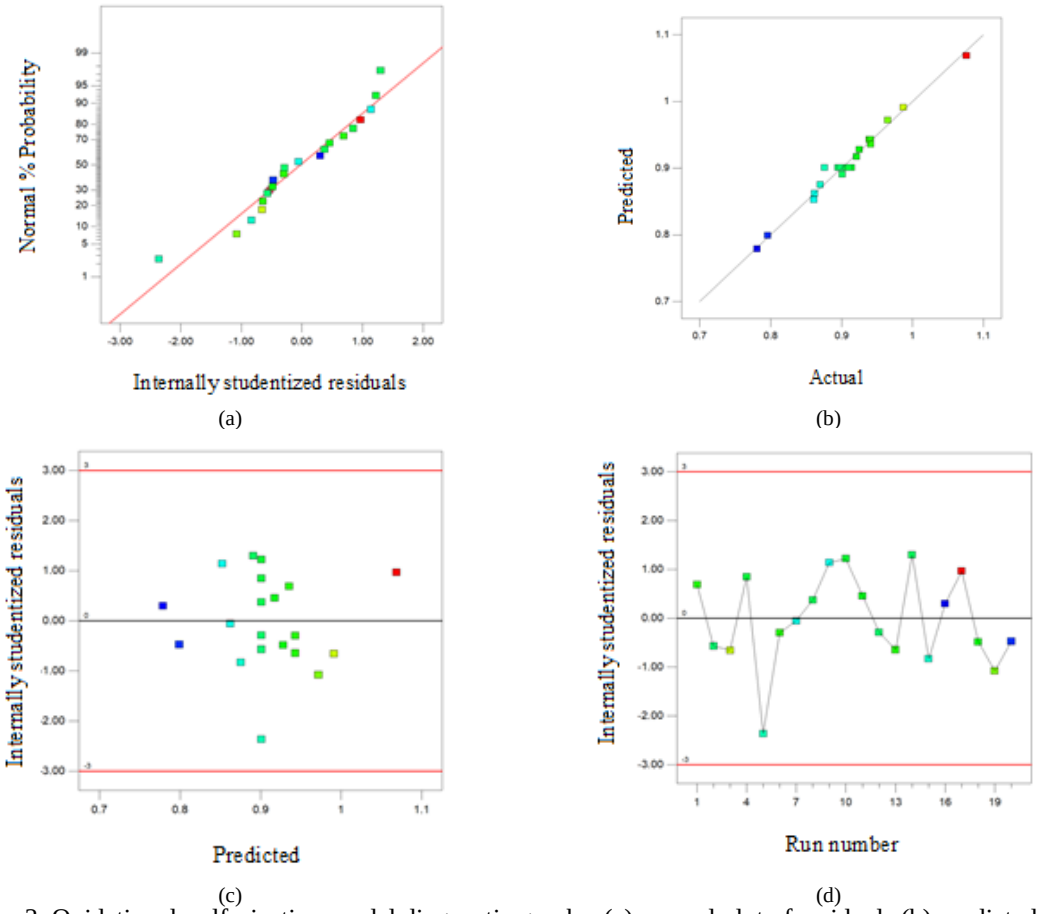

Figure 3. Oxidative desulfurization model diagnostic graphs; (a) normal plot of residuals (b) predicted versus actual (c) residuals versus predicted and (d) residuals versus the run number

3.2. Parameters effects

Single effects analysis

Model graphs make it possible to describe the outcomes of verified models. To analyze the link between parameters and the response, perturbation plots, all components' effects plots, and three-dimensional response surface plots may be employed.

Figure 4 depicts the perturbation plot. The response is plotted by varying one factor above and below its considered values while maintaining the other variables constant. The graph shows how each parameter affects the degree of oxidation at a particular reference point. Consequently, variations in the temperature and oxidant content of diesel fuel significantly impact the reaction.

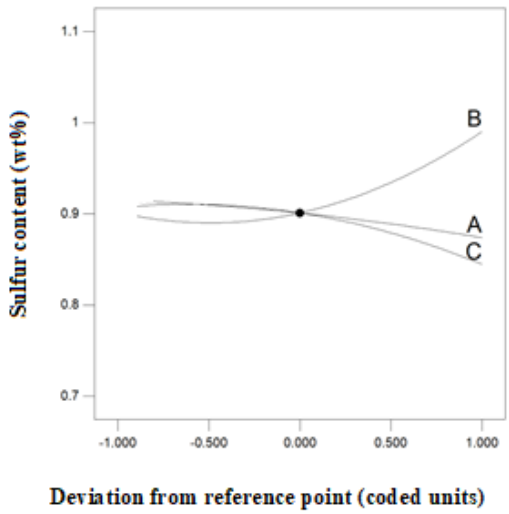

Figure 4. Perturbation plot of the parameters time (A), temperature (B), and oxidant % (C) in the design space.

Graphs of the one-factor effect are illustrated in Figure 5. The response indicates the linear impact of altering the level of each analyzed parameter as a result of the one-factor contribution analysis. The solid dots in the diagrams represent the experimental design

points. According to Figure 5a, as the oxidation time increased, the sulfur removal increased. When the time is altered from 20 to 90 minutes at 70ºC temperature and 12.5wt% oxidant, the sulfur content is reduced from 0.91wt% to 0.87wt%. The shift is due to enhanced contact between the two immiscible phases, which allows the oxidation process to occur and the transfer of polar oxidized sulfur compounds to the aqueous phase to be facilitated[45].

Figure 5b shows the influence of temperature on oxidative desulfurization at 55 minutes oxidation time and 12.5wt% oxidant. Sulfur content% reduced from 0.905 wt% to 0.890 wt% when the temperature is raised to 65°C. The response is quite sensitive in this region, and continuing to raise the temperature has a negative impact on desulfurization. Because the unsaturated hydrocarbons and nitrogen/oxygen-containing molecules are oxidized, potentially destroying oil quality and weakening oxidation selectivity. As a result, 65ºC is the ideal oxidation temperature.

A single impact study of acid to oxidant percent on oxidative desulfurization is displayed in Figure 5c. The oxidation time and temperature were fixed at 55 minutes, and 70 ºC respectively. The favorable impact of the acid to oxidant ratio on peracetic acid synthesis and activity is first seen to attain an optimum. The addition of acetic acid as a catalyst aids to the extraction of the oxidized sulfur compound from a polar media by promoting the synthesis of radical hydroperoxyl during the oxidation stage. According to the above results, electron cloud density and space steric hindrance significantly impact oxidative desulfurization. The constant rate K of the oxidation process rises as the density of the electron cloud of sulfur atoms increases. As a result, the oxidative desulfurization impact in dibenzothiophene must be substantially greater than in benzothiophene and thiophene[46]. Hydrogen peroxide represents the restrictive regent in oxidative desulfurization. Increases in its percentage lead to the formation of proxy-acid, then decomposition to active radicals in stoichiometry ratio[47]. Because of an adsorbital electron in the sulfur atom, peracetic acid's higher polarity selectively oxidizes sulfides to sulfoxide or sulfones. The sulfur atom bonds with oxygen atoms after oxidation, and the dipole moments of sulfur compounds increase, significantly improving their dissolving capacity in polar chemicals

Interactive effects analysis

Figure 6 shows graphical visualizations of the response surface plots. Each of these is sketched with a fixed value for one parameter at the center point and variations in two additional elements in the experimental inquiry ranges[44].

The interaction between oxidation time and temperature at the 12.5wt% oxidant in sulfuer removal% of the diesel fuel can be assessed using Figure 6a. Up to the optimum value, the beneficial effect is produced by parallel incrementing both parameters. The slow oxidation of sulfur compounds in diesel fuel to sulfoxide or sulfonic acid could be sped up by raising the temperature of the reaction. High temperatures enhance the kinetic energy of the reaction and increase the contact area for contributing moles. Because of peracetic acid breakdown, increasing the temperature of the reaction over 65ºC had a negative impact on the oxidation process[38]. So this treatment should be carried out at a cool temperature

Figure 6b depicts the interactive effect of oxidant percent and reaction duration at a constant temperature of 70ºC. The plots suggest that raising the oxidant percent with a longer reaction time has a less significant effect than increasing it with a shorter reaction time. Yet, the effect is still good for elimination. Time expedites the biphasic reaction and enhances elimination. Maximal sulfur oxidation occurred at 20 wt% oxidant .

At a fixed oxidation time of 55 minutes, Figure 6c demonstrates the mutual influence of temperature and oxidant concentration on sulfur content (wt%). As a result, the response is restricted to oxidant changes at lower temperatures. According to statistical modeling findings and parameter optimization, the best setting for oxidative desulfurization is a 12.5wt% oxidant at 65 ºC for 60 min of oxidation time

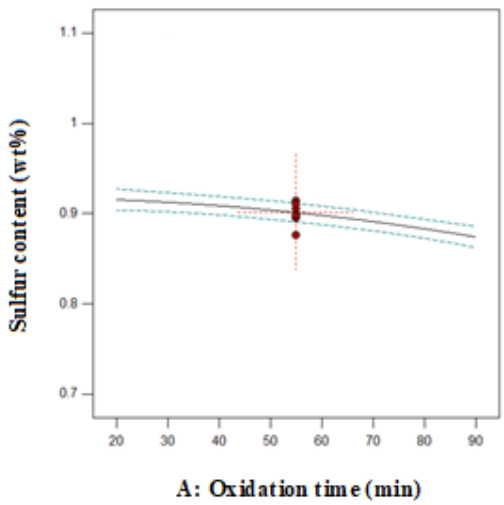

(a)

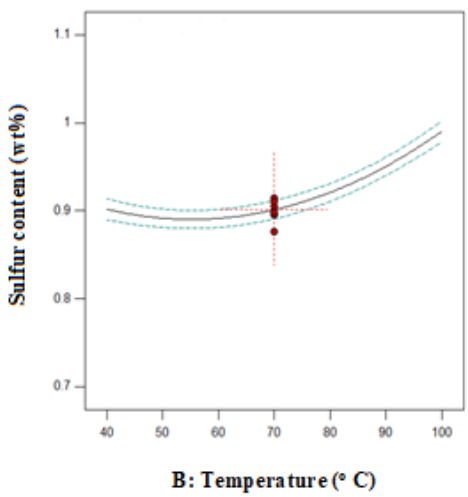

(b)

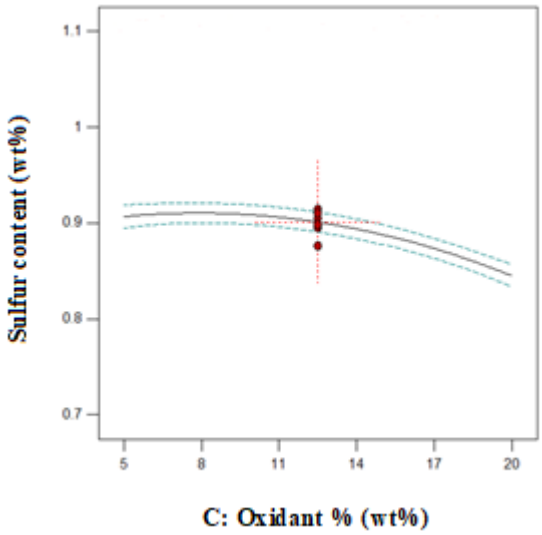

(c)

Figure 5. Influence of factors on the amount of desulfurization as a single factor; time(a), temperature(b), and oxidant%(c).

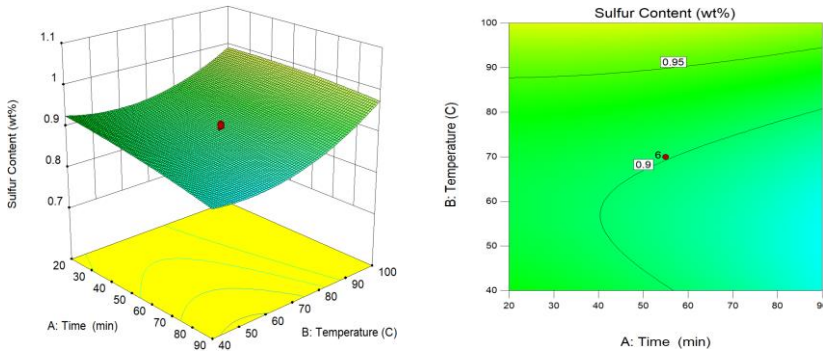

(a)

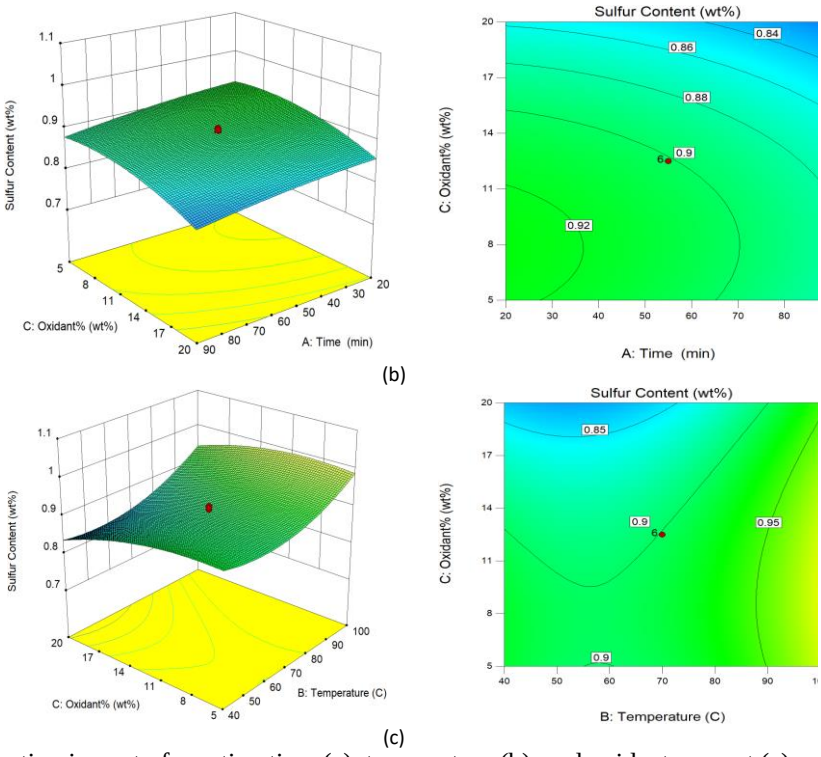

Figure 6. The interaction impact of reaction time (a), temperature (b), and oxidant percent (c) on desulfurization on a response surface 3-D graph..

4. Characterization of emulsified fuel

After oxidation of diesel fuel under the optimum condition in the previous step, several surfactants were used for emulsion preparation at the same quantity (2 wt% surfactants and 18 wt % 2-propanol) and terms (30 min, 25ºC, and 5000 rpm). Results of desulfurization by surfactants are shown in Table 7. As shown in Table 7, the Alkylbenzene sulfonate recorded less sulfur content (wt%).

Table 7. Desulfurization by different surfactants.

Surfactant	Symbol	Sulfur Content (wt%)
Cetyltrimethylammonium Chloride	CAC	0.666
Nonylphenol ethoxylates	NPE	0.644
Alkyl benzene sulfonate	ABS	0.598
Tween 80	T80	0.697
1-hyroxy-2-(trimethylammonio) ethane-1-sulfonate	HES	0.630

4.1. Effect of homogenizing time

The time of the homogenization process has a significant impact on the desulfurization process. Table 7 depicts the influence of homogenizing time on desulfurization efficiency. These experiments were conducted under the same conditions of 10000 rpm, 18% wt 2- propanol, 2% surfactant, and 30ºC.

During the first 10 minutes, it is evident that the emulsification efficiency on sulfur removal was low. The sulfur content (wt%) was lowered using ABS, CAC, and HES due to the variation in the homogenization time from 10 to 20 minutes. After 10 minutes of homogenization, T80 surfactants had an unfavorable effect, reduced after 30 minutes. The desulfurization rate of the NPE emulsifier was higher in the first 10 minutes; extra homogenizing time did not affect the desulfurization process. It may be determined using an NPE surfactant. Mass transfer equilibrium can be attained in under 10 minutes. The sulfur content of the CAC emulsifier was minimized until 30 minutes after homogenization. The emulsion deteriorated with time, increasing sulfur concentration. After 30 minutes of homogenizing, the emulsifier observes the least effect of time until a 30-

minute satisfactory result is attained, with a little increase in sulfur content content (wt%).

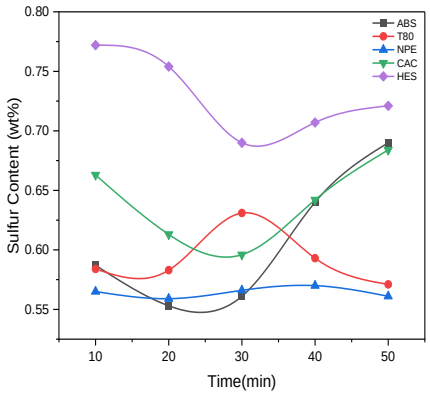

Figure 7. Impact of homogenization time on desulfurization efficiency.

4.2. Effect of homogenizing speed

Mainly, better mixing will obtain by high-speed homogenizing due to the formation of small droplets that allow increment of contact of the interfacial area, which enhances mixing quality[44, 48, 49]. The homogenising speed was changed from 5000 to 25000 rpm to investigate the influence of agitation on emulsification and the desulfurization process's performance. Figure 8 depicts the influence of surfactant homogenizing speed. In this step, experiments are done at 10 min, 18% wt% 2- propanol, 2% wt% surfactant, and 30°C.

The sulfur content (wt%) was decreased when mild speed homogenizing was used. Surfactants T80, NPE, and HES showed an approximate reduction in sulfur content until 5000 rpm; however, the increase in speed significantly affected the desulfurization rate. The formation of two separated phases at high speed and the separation of the formed emulsion at high speed. The optimum homogenizing speed for ABS and CAC surfactants was 15000 rpm because emulsified fuel recorded lower sulfur content (wt%) at this speed. More speed had the opposite effect on the desulfurization rate.

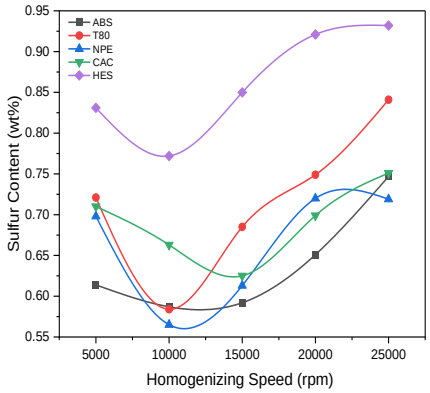

Figure 8. Effect of homogenizing speed on desulfurization rate.

4.3. Effect of reaction temperature

Many physical features, such as viscosities, interfacial tension, emulsifier adsorption, and the interfacial film structure between two liquids, are known to alter with temperature. Increasing the temperature reduces the stability of emulsions. When the temperature is raised, emulsion stability diminishes[44]. Figure 9 illustrates the impact of temperature on the desulfurization efficacy of the sulfur content. Under identical experimental operating conditions, the temperature ranged from 30 to 70 degrees Celsius. It's worth noting that better emulsification efficiencies can be attained at temperatures close to room temperature, which is more cost-effective. Except for the emulsifiers HES and CAC, the remainder of the surfactants (ABS, NPE, and T80) exhibited greater sulfur content when measured at temperatures over 40°C.

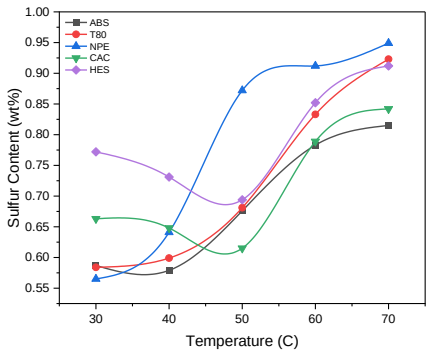

Figure 9. Impact of temperature on desulfurization rate.

4.4. Effect of co-surfactant concentration

In an attempt to further improve the sulfur removal, co-surfactants were introduced to the emulsified mixture. In this study ethanol was used as a co-surfactant with 2-propanol. Fig. 10 shows the sulfur removal performance due to the addition of ethanol. It seen that the adding ethanol to 2-propanol enhance the desulfurization performance. This may be due to the different chain lengths and the amount of hydrogen bonding functional moieties within the additives structure. [44]

Under optimal oxidation conditions, the sulfur content was reduced from 0.945 wt% to 0.781 wt%. It was evident from Figure 10 that ethanol reduced sulfur content by increasing its percent from 5% wt% to 30% wt% in emulsified diesel. However, 2-propanol showed higher activity toward desulfurization in emulsified fuels.

The temperature has a significant impact on the stability of emulsion. Higher temperatures boost the thermal an energy of the emulsion, resulting in more frequent drop collisions and larger drops, decreasing the total contact surface area between the fuel and the solvent and lowering mass transfer.

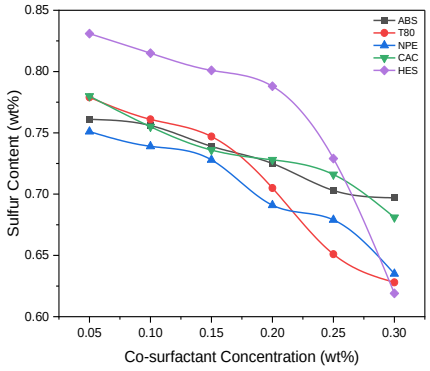

Figure 10. Influence of co-surfactant conc on desulfurization rate.

The influence of surfactant concentration on emulsification desulfurization is investigated in this study. After emulsification, the centrifuge method was used for separation the diesel fuel. However, amphoteric surfactant HES didn't separate by centrifuge in the absence of 2-propanol. The surfactants were added in different weight percentages (1% to 10%) to diesel fuel to study the effect of surfactant weight concentration on the sulfur removal ability. Figure 11 shows the influence of surfactant weight concentration on desulfurization process , as the surfactant concentration increased the sulfur content (wt%) decreased. This is due to the drop size and its dispersion significantly impact emulsion stability[36, 42, 43]. It was known that raising the surfactant concentration causes more surfactants to be absorbed in the interface and causes the emulsion to become stable. T80 and NPE surfactants performed similarl behaviour in the absence of co-surfactant, indicating the role of co-surfactant in the desulfurization process. Using a CAC emulsifier decreased the sulfur content (wt%) ,while increasing the concentration of ABS surfactant, resulting a slight decreased the sulfur content (wt%).

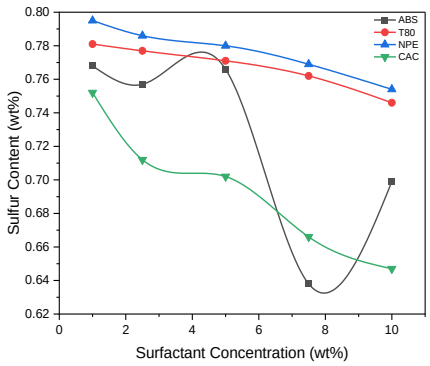

Figure 11. Influence of surfactant concentration on desulfurization rate.

It is widely understood that drop size and drops size dispersion significantly impact emulsion stability[44, 50, 51]. It was discovered that raising the surfactant concentration causes more surfactants to be absorbed in the interface and causes the emulsion to become stable. T80 and NPE surfactants performed similarly in the absence of co-surfactant, indicating the role of co-surfactant in the desulfurization rate. Using a CAC emulsifier increased the rate of desulfurization while increasing the concentration of ABS surfactant, resulting in a slight increase in sulfur content.

4.5. GC–MS analysis

GC–MS analysis was used to analyze the diesel fuel. Table 8 summarizes the outcomes. Mercaptan belongs to weak acid and thus can be oxidized easily to a disulfide. Peracetic acid is greatly affected by diesel fuel oxidization. After the oxidation process 1-propanethiol percent reduced 0.0624 to 0.020, both 2-Butanethiol and 2-Methyl-1-propaneth are disappeared in oxidized diesel fuel. After oxidation, the greatest sulfur compound in diesel fuel, 1-Butanethiol, is reduced by 97 percent, the largest decrease among other sulfur compounds. The

conversion of thiols to sulfides, which is removed by the emulsification process, creates hydrogen sulfides 0.2228 following oxidation. Due to the oxidation of other hydrocarbon compounds and the breaking of sulfur bonds from sulfur compounds in diesel fuel that did not convert to sulfides, total sulfur increased from 45.4426 to 47.0418. Table 7 shows that Alkylbenzene sulfonate has higher activity in reducing sulfur content and has the advantage of being inexpensive; hence it was chosen for the emulsification procedure. In the oxidation stage, hydrogen sulfides develop, easily eliminated by emulsion fuel. In the emulsion process, the trace of the remaining sulfur compound from the oxidation step is reduced. Total sulfur is decreased significantly in the emulsification stage, which pertains to the reactivity of produced sulfides and emulsified fuel trend sulfur component.

Table 8. Sulfur compounds and diesel fuel desulfurization rate.

No.	Compounds	Sulfur content / ppmw			Desulfurization rate%
		Diesel	After oxidation	After emulsification	
1	1-Propanethiol	0.0624	0.0280	0.0201	%67.78
2	2-Butanethiol	0.0383	0.0000	0.0000	%100
3	2-Methyl-1-propaneth	0.2308	0.0000	0.0000	%100
4	1-Butanethiol	2.9868	0.0885	0.0409	%98.63
5	H_2S	0.0000	0.2228	0.0000	%100
	Total	45.4426	47.0418	33.7720	%25.68

4.6. FT-IR analysis

After oxidation and desulfurization in the emulsification process, the FTIR spectrum of the diesel sample was obtained. As illustrated in Figure 12, it gives a better insight into the sorts of functional groups present in the samples. As demonstrated in Figure 12a, diesel fuel exhibited peaks of different intensities centered around 722.8–2955.37 cm-1. The significant alkyl C–H stretch was responsible for the peaks that occurred at 2854.30–3000 cm-1. The peak at 1459.14 cm-1 was assigned to aromatic compounds with a medium-strong ring C = C stretch, whereas the peak at 1377 cm-1 was attributed to alkanes and alkyls with a medium CH3C–H bend. Alkynes' strong wide C–H bend was credited with peaking at 722.8.

The existence of the C = O stretch, also known as the carboxylic group of peracetic acid, is responsible for the peaks of Figure 12b. in oxidized diesel fuel centered at 1716.13 cm-1. The disappearance of this peak following emulsification (Figure 12c) indicates a reaction of residual peracetic acid.

The strong, wide C– H bend of alkynes was ascribed to the peak centered at 699.02 cm-1, whereas modest cis C—H out-of-plane bending was assigned to the final two peaks at 785 and 766.26 cm-1.

4.7. IREX analysis

Table 9 shows the results of the IREX analysis for diesel fuel after oxidation and emulsification. Because of the presence of peracetic acid, the cetane number for net diesel fuel was higher than that of oxidized diesel fuel (23.2). The cetane number of emulsified fuel increased by 23.8. Diesel fuel oxidation was reduced from 13.5 to 3.3 aromatics, while emulsified fuel oxidation was reduced to 0.0.

Table 9. IREX analysis of diesel fuel.

NO.	Parameters	Diesel fuel (Vol%)	After oxidation (Vol%)	After emulsification (Vol%)
1.	Cetane Number	34.7	23.2	23.8
2.	Aromatics	13.5	3.3	0
3.	PNA	4	4.3	5.4
4.	FAME	0	3.07	0.11
5.	IBP	162	288.8	172.8
6.	T50	248.7	232.5	288.3
7.	FBP	358.7	261	478.7

The increments in polynuclear aromatic compounds (PNA) in emulsified and oxidized diesel fuel were recorded at 5.4 and 4.3, respectively. These increments were due to the presence of non-linear hydrocarbons compared to the net diesel fuel PNA 4.

After oxidation of the diesel fuel, fatty acid methyl ester (FAME) exhibited the highest value of 3.07 due to the presence of ester bonds. It is formed by the reaction of the hydroxyl group (O-H) in hydrogen peroxide with the carbonyl group (C=O) in acetic acid that has a hydroxyl group (O-H) attached to the carbon atom.

FAME in net diesel fuel was 0.0, but after emulsification, it was reduced to 0.11 due to the removal of excess peracetic acid and water. The path of diesel fuel boiling has changed due to changes in fuel components. An increment in IBP was noticed after oxidation from 162 ^{o}C to 288.8 ^{o}C. This increase in IBP was traced back to the presence of a carboxylic group (C(=O) OH) in peracetic acid, which contains hydrogen bonding and sulfur compound oxidation. Emulsified fuel reduced IBP to 172.8 ^{o}C by removing oxidized sulfur compounds, whereas a centrifuge separates the remaining unreacted peracetic acid.

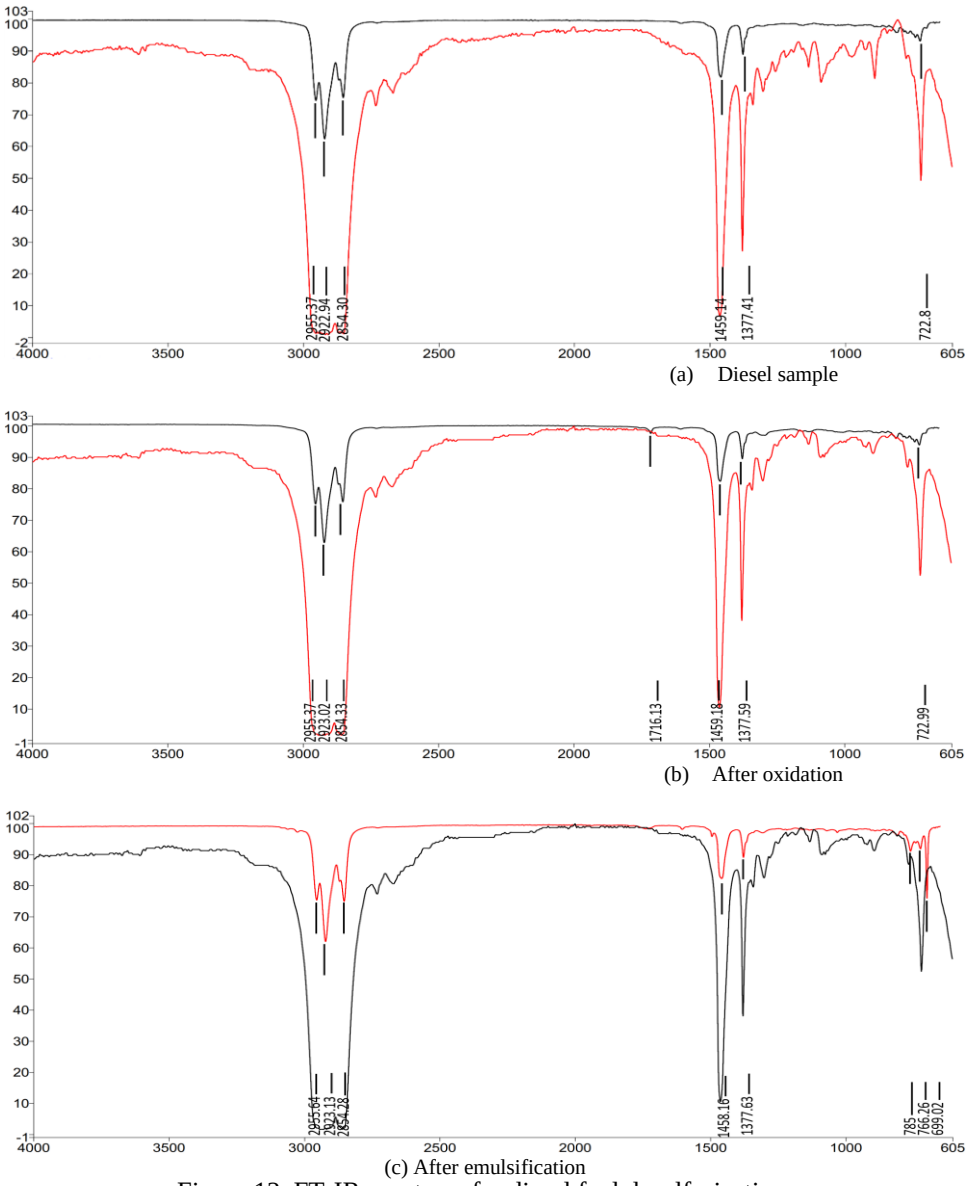

Figure 12. FT-IR spectrum for diesel fuel desulfurization.

5. Conclusion

In the current study, the desulfurization of diesel with an initial sulfur content of 0.945 wt.% was investigated utilizing a mix of oxidation-emulsification processes. This technique is a viable desulfurization alternative with a lot of potential and low cost for industrial applications. For the oxidation of sulfur compounds in diesel fuel, a 2:1 mixture of H_2O_2 and acetic acid was utilized as an oxidizing agent. The input variables were optimized using the "Response Surface Methodology (RSM)" depending on the efficiency of the output results. According to the results of CCD design, oxidation at a 12.5 wt % oxidant ratio and 65 °C for 60 minutes resulted in an optimal desulfurization rate of 17.35 wt percent. The sulfur content increased when the oxidation process temperature was raised above 70°C, the sulfur content increased. The presence of surfactants aids the rate of desulfurization. The effect of homogenizing time may be restricted to 10–30 minutes, while surfactants used for longer than 30 minutes had no adverse effects. To remove sulfur from emulsified fuel, a low reaction temperature was chosen. The desulfurization rate was greatly boosted when alcohol was used as a co-surfactant. 2-propanol was more effective than ethanol at desulfurization.

6. References

[1]. Chu S., Zhou W., Zhang C., Zheng Y., Liu Y., and Liu Y., Relationship between the structure and catalytic performance of MoS2 with different surfactant-assisted syntheses in the hydrodesulfurization reaction of 4,6-DMDBT. *RSC Advances*. **10**(13): p. 7600-7608(2020)

[2]. Fan L. and Gu B., Impacts of the Increasingly Strict Sulfur Limit on Compliance Option Choices: The Case Study of Chinese SECA. *Sustainability*. **12**(1): p. 165(2020)

[3]. Svinterikos E., Zuburtikudis I., and Al-Marzouqi M., Carbon Nanomaterials for the Adsorptive Desulfurization of Fuels. *Journal of Nanotechnology*. **2019**: p. 2809867(2019)

[4]. Ahmad W., Sulfur in Petroleum, in *Applying Nanotechnology to the Desulfurization Process in Petroleum Engineering*, T.A. Saleh, Editor. 2016, IGI Global: USA. p. 523

[5]. Milbourn C. EPA Gives the Green Light on Diesel Sulfur Rule. 2001 [cited 2022 10 Jan.]; Available from: https://archive.epa.gov/epapages/newsroom_archive/newsreleases/0237f756e256922c85256a010072e4f6.html.

[6]. Regulatory Impact Analysis: Heavy-duty Engine and Vehicle Standards and Highway Diesel Fuel Sulfur Control Requirements. 2000: Environmental Protection Agency EPA420-R-00-026.

[7]. Zeng X., Wang H., DeYonker N. J., Mo G., Zhou R., and Zhao C., Reaction mechanism of oxidative desulfurization of heterocyclic organic sulfides: a computational study. *Theoretical Chemistry Accounts*. **133**: p. 1-6(2014)

[8]. Yuan P., Lei X.-Q., Sun H.-M., Zhang H.-W., Cui C.-S., Yue Y.-Y., Liu H.-Y., Bao X.-J., and Wang T.-H., Effects of pore size, mesostructure and aluminum modification on FDU-12 supported NiMo catalysts for hydrodesulfurization. *Petroleum Science*. **17**(6): p. 1737-1751(2020)

[9]. Yang L., Li X., Wang A., Prins R., Chen Y., and Duan X., Hydrodesulfurization of dibenzothiophene, 4,6-dimethyldibenzothiophene, and their hydrogenated intermediates over bulk tungsten phosphide. *Journal of Catalysis*. **330**: p. 330-343(2015)

[10]. Hossain M. N., Park H. C., and Choi H. S., A Comprehensive Review on Catalytic Oxidative Desulfurization of Liquid Fuel Oil. *Catalysts*. **9**(3): p. 229(2019)

[11]. Zhu W., Zhu G., Li H., Chao Y., Zhang M., Du D., Wang Q., and Zhao Z., Catalytic kinetics of oxidative desulfurization with surfactant-type polyoxometalate-based ionic liquids. *Fuel Processing Technology*. **106**: p. 70-76(2013)

[12]. Rajendran A., Cui T.-y., Fan H.-x., Yang Z.-f., Feng J., and Li W.-y., A comprehensive review on oxidative desulfurization catalysts targeting clean energy and environment. *Journal of Materials Chemistry A*. **8**(5): p. 2246-2285(2020)

[13]. Flores R., Rodas A., and Gasperin R., Oxidative desulfurization of diesel fuel oil using supported Fenton catalysts and assisted with ultrasonic energy. *Petroleum Science*. **16**(5): p. 1176-1184(2019)

[14]. Sachdeva T. and Pant K., Deep desulfurization of diesel via peroxide oxidation using phosphotungstic acid as phase transfer catalyst. *Fuel Processing Technology*. **91**(9): p. 1133-1138(2010)

[15]. Mondal S., Hangun-Balkir Y., Alexandrova L., Link D., Howard B., Zandhuis P., Cugini A., Horwitz C. P., and Collins T. J., Oxidation of sulfur components in diesel fuel using Fe-TAML® catalysts and hydrogen peroxide. *Catalysis Today*. **116**(4): p. 554-561(2006)

[16]. Wang D., Qian E. W., Amano H., Okata K., Ishihara A., and Kabe T., Oxidative desulfurization of fuel oil: Part I. Oxidation of dibenzothiophenes using tert-butyl hydroperoxide. *Applied Catalysis A: General*. **253**(1): p. 91-99(2003)

[17]. Collins F. M., Lucy A. R., and Sharp C., Oxidative desulphurisation of oils via hydrogen peroxide and heteropolyanion catalysis. *Journal of Molecular Catalysis A: Chemical*. **117**(1-3): p. 397-403(1997)

[18]. Gao J., Wang S., Jiang Z., Lu H., Yang Y., Jing F., and Li C., Deep desulfurization from fuel oil via selective oxidation using an amphiphilic peroxotungsten catalyst assembled in emulsion droplets. *Journal of Molecular Catalysis A: Chemical*. **258**(1-2): p. 261-266(2006)

[19]. Kairbekov Z. K., Myltykbaeva Z. K., Muktaly D., Nysanova B., Anisimov A., and Akopyan A., Peroxide oxidative desulfurization of a diesel fuel. *Theoretical Foundations of Chemical Engineering*. **52**(4): p. 677-680(2018)

[20]. Joskic R., Margeta D., and Bionda K. S., Oxidative desulfurization of model diesel fuel with hydrogen peroxide. *Goriva i maziva*. **53**(1): p. 11(2014)

[21]. Al-Moameri H. H., Hassan G., and Abdulrehman M. A., Predicting the composition of qurna crude oil fraction by ternary composition diagram. *Methods and Objects of Chemical Analysis*. **15**(1): p. 33-39(2020)

[22]. Zhang Q., Zhou M., Ren G., Li Y., Li Y., and Du X., Highly efficient electrosynthesis of hydrogen peroxide on a superhydrophobic three-phase interface by natural air diffusion. *Nature Communications*. **11**(1): p. 1731(2020)

[23]. Mazanov S. V., Aetov A. U., Usmanov R. A., Gabitov R. R., Zaripov Z. I., and Gumerov F. M., Oxidation of Acetic Acid by Hydrogen Peroxide in the Aqueous Medium in Supercritical Fluid Conditions. *Russian Journal of Physical Chemistry B*. **13**(7): p. 1131-1134(2019)

[24]. Al Otaibi R. L., Liu D., Hou X., Song L., Li Q., Li M., Almigrin H. O., and Yan Z., Desulfurization of Saudi Arabian crudes by oxidation-extraction method. *Appl Petrochem Res*. **5**(4): p. 355-362(2015)

[25]. Kang J. and Park E. D., Selective Oxidation of Methane over Fe-Zeolites by In Situ Generated H2O2. *Catalysts*. **10**(3): p. 299(2020)

[26]. da Silva M. J., de Andrade Leles L. C., Natalino R., Ferreira S. O., and Coronel N. C., An Efficient Benzaldehyde Oxidation by Hydrogen Peroxide over Metal Substituted Lacunary Potassium Heteropolyacid Salts. *Catalysis Letters*. **148**: p. 1202+(2018)

[27]. Menegazzo F., Signoretto M., Ghedini E., and Strukul G., Looking for the "Dream Catalyst" for Hydrogen Peroxide Production from Hydrogen and Oxygen. *Catalysts*. **9**(3): p. 251(2019)

[28]. Babahydari A. K., Fareghi-Alamdari R., Hafshejani S. M., Rudbari H. A., and Farsani M. R., Heterogeneous oxidation of alcohols with hydrogen peroxide catalyzed by polyoxometalate metal–organic framework. *Journal of the Iranian Chemical Society*. **13**(8): p. 1463-1470(2016)

[29]. Mirante F., de Castro B., M. Granadeiro C., and S. Balula S., Solvent-Free Desulfurization System to Produce Low-Sulfur Diesel Using Hybrid Monovacant Keggin-Type Catalyst. *Molecules*. **25**(21): p. 4961(2020)

[30]. Allahresani A., Naghdi E., Nasseri M. A., and Hemmat K., Selective oxidation of alcohols and sulfides via O2 using a Co(ii) salen complex catalyst immobilized on KCC-1: synthesis and kinetic study. *RSC Advances*. **10**(62): p. 37974-37981(2020)

[31]. Peckh K., Lisicki D., Talik G., and Orlińska B., Oxidation of Long-Chain α-Olefins Using Environmentally-Friendly Oxidants. *Materials*. **13**(20): p. 4545(2020)

[32]. Lyu J., Niu L., Shen F., Wei J., Xiang Y., Yu Z., Zhang G., Ding C., Huang Y., and Li X., In Situ Hydrogen Peroxide Production for Selective Oxidation of Benzyl Alcohol over a Pd@Hierarchical Titanium Silicalite Catalyst. *ACS Omega*. **5**(27): p. 16865-16874(2020)

[33]. Gordon C. P., Engler H., Tragl A. S., Plodinec M., Lunkenbein T., Berkessel A., Teles J. H., Parvulescu A.-N., and Copéret C., Efficient epoxidation over dinuclear sites in titanium silicalite-1. *Nature*. **586**(7831): p. 708-713(2020)

[34]. Xu Y., Liu Y., Xie H., Chen M., and Wang L., Experimental Study on Organic Sulfur Removal in Bituminous Coal by a 1-Carboxymethyl-3-methyl Imidazolium Bisulfate Ionic Liquid and Hydrogen Peroxide Solution. *ACS Omega*. **5**(33): p. 21127-21136(2020)

[35]. Xu Y., Liu Y., Bu Y., Chen M., and Wang L., Review on the ionic liquids affecting the desulfurization of coal by chemical agents. *Journal of Cleaner Production*. **284**: p. 124788(2021)

[36]. José da Silva M. and Faria dos Santos L., Novel Oxidative Desulfurization of a Model Fuel with H₂O₂ Catalyzed by AlPMo₁₂O₄₀ under Phase Transfer Catalyst-Free Conditions. *Journal of Applied Chemistry*. **2013**: p. 147945(2013)

[37]. Rivoira L. P., Martínez M. L., Falcón H., Beltramone A. R., Campos-Martin J. M., Fierro J. L. G., and Tartaj P., Probing the Catalytic Activity of Sulfate-Derived Pristine and Post-Treated Porous TiO2(101) Anatase Mesocrystals by the Oxidative Desulfurization of Dibenzothiophenes. *ACS Omega*. **2**(5): p. 2351-2359(2017)

[38]. Kunigk L., Gomes D., Forte F., Vidal K., Gomes L., and Sousa P., The influence of temperature on the decomposition kinetics of peracetic acid in solutions. *Brazilian Journal of Chemical Engineering*. **18**: p. 217-220(2001)

[39]. Tartaro G., Mateos H., Schirone D., Angelico R., and Palazzo G., Microemulsion Microstructure(s): A Tutorial Review. *Nanomaterials (Basel)*. **10**(9)(2020)

[40]. Ashikhmin A., Piskunov M., Yanovsky V., and Yan W.-M., Properties and Phase Behavior of Water-in-Diesel Microemulsion Fuels Stabilized by Nonionic Surfactants in Combination with Aliphatic Alcohol. *Energy & Fuels*. **34**(2): p. 2135-2142(2020)

[41]. Santos F. K. G., Neto E. L. B., Moura M. C. P. A., Dantas T. N. C., and Neto A. A. D., Molecular behavior of ionic and nonionic surfactants in saline medium. *Colloids and Surfaces A: Physicochemical and Engineering Aspects*. **333**(1): p. 156-162(2009)

[42]. Mjalli F. S., Rahma W. S. A., Al-Wahaibi T., and Al-Hashmi A. A., Superior liquid fuel desulfurization through emulsification solvent extraction using polymeric-based eutectic solvents. *Chinese Journal of Chemical Engineering*, (2019)

[43]. Nam S. N. a., Cho H., Han J., Her N., and Yoon J., Photocatalytic degradation of acesulfame K: Optimization using the Box-Behnken design (BBD). *Process Safety and Environmental Protection*. **113**: p. 10-21(2018)

[44]. B. Dawood N., A. AbdulRazak A., and S. Hamadi A., Optimizing Nano Metalworking Emulsions Preparation Using Response Surface Method. *Engineering and Technology Journal*. **39**(2A): p. 214-232(2021)

[45]. Ja'fari M., Ebrahimi S. L., and Khosravi-Nikou M. R., Ultrasound-assisted oxidative desulfurization and denitrogenation of liquid hydrocarbon fuels: A critical review. *Ultrasonics Sonochemistry*. **40**: p. 955-968(2018)

[46]. Otsuki S., Nonaka T., Takashima N., Qian W., Ishihara A., Imai T., and Kabe T., Oxidative Desulfurization of Light Gas Oil and Vacuum Gas Oil by Oxidation and Solvent Extraction. *Energy & Fuels*. **14**(6): p. 1232-1239(2000)

[47]. Bhasarkar J. B., Chakma S., and Moholkar V. S., Mechanistic Features of Oxidative Desulfurization Using Sono-Fenton–Peracetic Acid (Ultrasound/Fe2+–CH3COOH–H2O2) System. *Industrial & Engineering Chemistry Research*. **52**(26): p. 9038-9047(2013)

[48]. Mokhtar W. N. A. W., Bakar W. A. W. A., Ali R., and Kadir A. A. A., Deep desulfurization of model diesel by extraction with N,N-dimethylformamide: Optimization by Box–Behnken design. *Journal of the Taiwan Institute of Chemical Engineers*. **45**(4): p. 1542-1548(2014)

[49]. Tamminen J., Sainio T., and Paatero E., Intensification of metal extraction with high-shear mixing. *Chemical Engineering and Processing: Process Intensification*. **73**: p. 119-128(2013)

[50]. Goodarzi F. and Zendehboudi S., A Comprehensive Review on Emulsions and Emulsion Stability in Chemical and Energy Industries. *The Canadian Journal of Chemical Engineering*. **97**(1): p. 281-309(2019)

[51]. Fallah F., Khorasani M., and Ebrahimi M., Comparative study of gel emulsification and direct mechanical emulsification methods. *Colloids and Surfaces A: Physicochemical and Engineering Aspects*. **492**: p. 207-212(2016)